

Probing Primordial Stochastic Gravitational Wave Background with Multi-band Astrophysical Foreground Cleaning

Zhen Pan^{1,*} and Huan Yang^{1,2,†}

¹*Perimeter Institute for Theoretical Physics, Ontario, N2L 2Y5, Canada*

²*University of Guelph, Guelph, Ontario N2L 3G1, Canada*

(Dated: January 10, 2020)

The primordial stochastic gravitational wave background (SGWB) carries first-hand messages of early-universe physics, possibly including effects from inflation, preheating, cosmic strings, electroweak symmetry breaking, and etc. However, the astrophysical foreground from compact binaries may mask the SGWB, introducing difficulties in detecting the signal and measuring it accurately. In this Letter, we propose a foreground cleaning method taking advantage of gravitational wave observations in other frequency bands. We apply this method to probing the SGWB with space-borne gravitational wave detectors, such as the Laser Interferometer Space Antenna (LISA). We find that the spectral density of the LISA-band astrophysical foreground can be predicted with percent-level accuracy assuming 10-years' observations of third-generation GW detectors, e.g., Cosmic Explorer. After the foreground cleaning, LISA's sensitivity to the primordial SGWB will be substantially improved.

Introduction.— Primordial stochastic gravitational wave background (SGWB) has been conjectured to arise from various fundamental physical processes from the early universe [see e.g. Refs. 1, 2, for recent reviews], including the inflationary origin [3–10], cosmic strings [e.g., 11–22] and first-order phase transition due to electroweak symmetry breaking [e.g., 23–30]. Therefore measuring primordial SGWB at different frequencies will provide important information to understand our universe before recombination [31–37]. However, the total SGWB also contains contribution from astrophysical foreground of gravitational waves (GWs) from unresolved compact binaries [36, 38–44], including binary white dwarfs (BWDs), binary black holes (BBHs), binary neutron stars (BNSs) and possibly black hole-neutron star binaries (BHNSs). Removing the influence by the astrophysical foreground would be an essential step towards the measurements of primordial SGWB.

Inspired by recent discussions about the benefits of multi-band GW observations [45–52], we propose a multi-band foreground cleaning method and apply it to measuring the primordial SGWB in the LISA band [53]. The third-generation GW detectors, e.g. Cosmic Explorer (CE) [54] and Einstein Telescope (ET) [55], are expected to detect almost all BBH and BNS mergers in our universe [56, 57]. With data from these ground-based detectors, we can reconstruct the underlying distribution of the BBH/BNS population and derive their contribution to the astrophysical foreground in the LISA band. In particular, we find that the astrophysical foreground can be predicted with percent-level accuracy with the CE running for 10 years. After removing this predicted astrophysical foreground from the LISA data, it can be shown that LISA's sensitivity to the primordial SGWB will be substantially enhanced.

In this work, we use BBHs as the proxy of astrophysical foreground sources, while the astrophysical foreground

sourced by BNSs and BHNSs can be cleaned in the same way. This multi-band foreground cleaning method does not apply for the galactic BWDs, because BWDs merge at a much lower frequency and never enter the band of ground-based detectors. Therefore we conservatively confine our analysis to a higher frequency band ($f \gtrsim 5$ mHz) where the galactic BWDs can be completely resolved by LISA [58].

We use the geometrical units $G = c = 1$ and assume a flat Λ CDM cosmology with $H_0 = 70$ km/s/Mpc, $\Omega_\Lambda = 0.7$ and $\Omega_m = 0.3$.

Stochastic GWs from BBHs.— We now elaborate how to estimate the BBH foreground in the LISA band given a sample of BBH mergers detected by the CE. Consider an observational period of LISA in $[-T/2, T/2]$, the average spectral density of the BBH foreground in this period is (see Appendix)

$$\hat{H}_A(f) = \frac{1}{T} \sum_i (|h_+(f)|^2 + |h_\times(f)|^2)_i \Theta_T^i(f), \quad (1)$$

where index i runs over all BBHs in our universe, $\Theta_T^i(f) = 1$ if $f \in [f_{t=-T/2}^i, f_{t=T/2}^i]$ and $\Theta_T^i(f) = 0$ otherwise. Here f_t^i denotes the frequency of GW emitted at time t from i -th BBH, so that during the LISA observational period, only BBHs that cross the frequency f contribute to the summation in Eq. (1). In the quasi-circular approximation, one can show that the expectation value of $\hat{H}_A(f)$ is

$$\langle \hat{H}_A(f) \rangle = \dot{N}_O \frac{f^{-7/3}}{6\pi^{4/3}} \int_0^\infty P(\zeta) \zeta^2 d\zeta, \quad (2)$$

where $\langle \dots \rangle$ is the ensemble average over realizations of BBHs, \dot{N}_O is the merger rate seen in the observer's frame (i.e., number of mergers per unit time detected by CE/ET), $\zeta := (GM_z)^{5/6}/D_L$ and $P(\zeta)$ is

the corresponding distribution function normalized as $\int_0^\infty P(\zeta)d\zeta = 1$, with $\mathcal{M}_z = (1+z)M_c$ being the redshifted chirp mass, and D_L being the luminosity distance.

Physically Eqs. (1) and (2) display two different perspectives in understanding the astrophysical foreground. The former describes an event-based approach: the foreground consists of GWs from all unresolved (by the LISA) inspiral binaries, each of which will enter the ground detector band at a later time; therefore the foreground may be estimated by summing up contribution from events later identified by CE or ET. Eq. (2) states that the (ensemble average of) foreground can be obtained from the statistical distribution of the BBHs, which may also be measured precisely by ground-based detectors. While both approaches are equivalent given infinite detector running time and accuracy (see Appendix), we will show later that the distribution-based approach is much more efficient than the event-to-event subtraction given a finite detector running time, say 10 years. In the following sections, we will adopt the distribution-based approach and briefly discuss the application of Eq. (1) in an event-to-event subtraction in the Supplemental Material.

To describe the underlying distribution of the BBH mergers, we need to specify the local merger rate density $R(z)$ (number of mergers per comoving volume per unit of cosmic time) and the mass distribution $p(m_1, m_2)$. As a fiducial model, we assume $R(z) = R_0 e^{-(z/10)^2}$ with $R_0 = 65 \text{ Gpc}^{-3}\text{yr}^{-1}$ [59], and

$$p(m_1, m_2) \propto \frac{1}{m_1(m_1 - m_{\min})}, \quad (3)$$

for $m_{\min} \leq m_2 \leq m_1 \leq m_{\max}$, with $m_{\min} = 5M_\odot$ and $m_{\max} = 42M_\odot$. Combining the mass distribution $p(m_1, m_2)$ with the merge rate density $R(z)$, it is straightforward to infer the merger rate \dot{N}_O in the observer's frame and the underlying distribution function $P(\zeta)$ (see Fig. 1). Given $R(z)$ and $p(m_1, m_2)$, we also generate many samples of BBH mergers. We then reconstruct the distribution function $P(\zeta)$ assuming a number of merger events are recorded by ground-based detectors.

Distribution Reconstruction.— We model the Fourier-domain waveform $h_A(f)$ of BBH mergers with the PhenomB waveform [60] which depends on 7 parameters: redshifted chirp mass \mathcal{M}_z , redshifted total mass M_z , luminosity distance D_L , effective spin χ , merger time t_0 , merger phase φ_0 and inclination angle ι . The measured strain $h(f)$ is related to $h_A(f)$ by

$$h(f) = h_+(f)F^+(f; \theta, \phi, \psi) + h_\times(f)F^\times(f; \theta, \phi, \psi), \quad (4)$$

where $F^{+, \times}(f; \theta, \phi, \psi)$ are the detector response functions which depend on the sky location θ, ϕ and the polarization angle ψ . As an example, we consider a network with three detectors (assuming CE sensitivity) located

TABLE I. Location and orientation of the three ground-based detectors considered in this work.

	latitude	longitude	orientation
Detector 1	32° S	115° E	135°
Detector 2	38° N	104° E	90°
Detector 3	31° N	90° W	27°

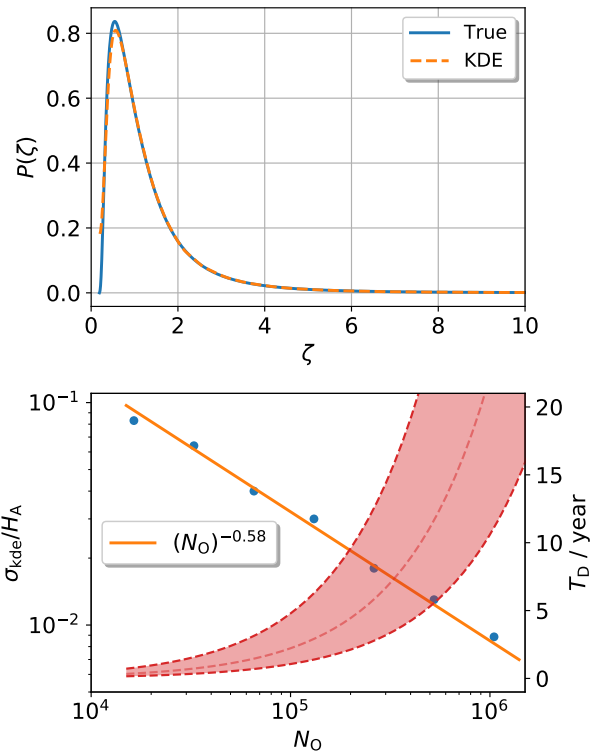


FIG. 1. Upper panel: the solid line is the underlying distribution of ζ defined following Eq. (2), and the dashed line is the KDE reconstruction from 4.5×10^5 merger events detected by the detector network, where ζ is shown in units of $M_\odot^{5/6} \text{Gpc}^{-1}$. Lower panel: the dots denote the fractional deviation of KDE reconstructed SGWB spectral density and the solid line is a power-law fit $\sigma_{\text{kde}}/H_A \propto N_O^{-0.58}$. The shadowed area denotes the uncertainty in the amount of mergers we expect the ground-based detectors to record in a given running time T_D , where the thin/dashed line in the center is the fiducial model we use in this work and the two thick/dashed lines correspond to merger rate density $R_0 = 65^{+75}_{-34} \text{ Gpc}^{-3}\text{yr}^{-1}$ [59].

in Australia, China and US respectively, with their locations and arm orientations specified in Table I, where the orientation is the angle between the bisector of two detector arms and the local west-to-east direction.

For each event, we estimate the parameter uncertainties using the Fisher matrix,

$$F_{\alpha\beta} = \sum_{d=1}^3 F_{\alpha\beta}^d = \sum_{d=1}^3 4 \int_0^\infty \frac{\Re[h_{d,\alpha}(f)h_{d,\beta}^*(f)]}{P_n(f)} df, \quad (5)$$

where \Re denotes the real part, $h_d(f)$ is the strain in detector d , $h_{d,\alpha}$ is the derivative with respect to parameter α , and $P_n(f)$ is the noise spectral density of detectors [54]. The $1\text{-}\sigma$ uncertainty of parameter α is given by $\sigma_\alpha = \sqrt{(F^{-1})_{\alpha\alpha}}$. During an observational period T_D , we observe N_O mergers together with their best-estimated parameters $\{\zeta_i\}$ ($i = 1, \dots, N_O$), where ζ_i is sampled from a Gaussian distribution with mean value ζ_i^{true} and standard deviation $\sqrt{\zeta_{i,\alpha}(F^{-1})_{\alpha\beta}\zeta_{i,\beta}}$.

With a sample of $\{\zeta_i\}$, we can estimate the underlying distribution $P(\zeta)$ using the kernel density estimator (KDE). We make use of the FFTKDE module from Python package KDEpy and determine the estimator bandwidth using Silverman's rule of thumb [61]. In Figure 1, we show the KDE reconstructed distribution function $P(\zeta)$ from a sample of 4.5×10^5 data points. The underlying distribution is reconstructed to a good precision except in the range of small ζ [62].

To quantify the performance of the KDE reconstruction, we generate 100 realizations of N_O BBH mergers, "observe" each merger with the detector network and reconstruct $P(\zeta)$ in each realization. With the reconstructed $P(\zeta)$, we then calculate the spectral density $H_{\text{kde}}(f)$ using Eq. (2). In Fig. 1, we show the fractional deviation $\sigma_{\text{kde}}/H_A := \sqrt{\langle (H_{\text{kde}} - H_A)^2 \rangle}/H_A$ as a function of the total number of mergers N_O . We find that the fractional bias scales as $\propto N_O^{-0.58}$, being $\sim 1.3\%$ for $N_O = 4.5 \times 10^5$ which is roughly the number of BBH merger events in 10 years.

Estimating the Extragalactic BWD Foreground.— Starting from the mHz range the galactic BWDs will be resolved by LISA, so that the main sources of SGWs are extragalactic BWDs [38] and compact binaries (BBHs, BNSs, and BHNSs) [63]. As the compact binary foreground can be estimated with ground-based GW detections and cleaned accordingly, let us examine the detection of SGWs from extragalactic BWDs in the absence of primordial waves. For simplicity, let us consider two LISA detectors with output $s_d(t) = h_d(t) + n_d(t)$ ($d = 1, 2$), with h_d and n_d denoting the gravitational strain and the intrinsic noise in detector d , respectively. The case with a single detector is discussed in the Appendix, along with details on constructing the SGWs estimators.

In the upper panel Fig. 2, we present the spectral densities of LISA detector noise, stochastic GW foreground from various sources, and the residual foreground ($\sigma_{\text{kde}}/H_A = 1.3\%$) of compact binaries. In the lower panel, we show the SNRs of extragalactic BWD SGWs with spectral density $H_{\text{BWD}}^{\text{ext}}(f)$ [38, 58]. Notice that without the compact binary foreground cleaning, the BWD background can still be computed by utilizing the spectral shape of the foreground (see Appendix), albeit with much worse sensitivity. Such comparison is shown by the two dashed lines in the figure, where the fore-

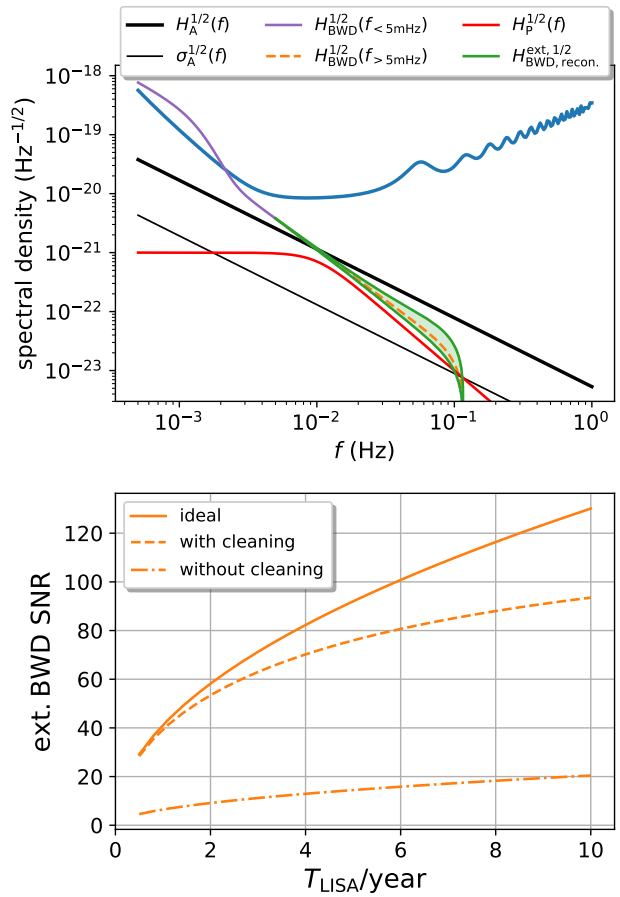


FIG. 2. Measuring the SGWs from extragalactic BWDs $H_{\text{BWD}}^{\text{ext}}(f)$. Upper panel: the spectral densities of effective LISA detector noise $S_n(f)$ (blue), BBH foreground $H_A(f)$ (thick black) and residual foreground $\sigma_A(f)$ after cleaning (thin black), unresolved low-frequency/high-frequency BWD foreground $H_{\text{BWD}}(f)$ (purple/orange) [38, 58, 64], and reconstructed high-frequency BWD foreground $H_{\text{BWD}}^{\text{ext}}(f)$ (green shadow), and a primordial SGWB $H_P(f)$ from [65] (red). Lower panel: SNRs of different estimators for the high-frequency extragalactic BWD foreground, where the BBH foreground cleaning increases the detection sensitivity by a factor 4 \sim 7. We also examined less optimistic scenarios of foreground cleaning with 2 CE-like detectors, and we find the SNR (dashed line) decreases by maximally $\sim 15\%$.

ground cleaning increases the detection sensitivity by a factor of 4 \sim 7. In the same figure, the solid line depicts the SNR of an ideal case assuming there was no foreground contamination from compact binaries.

With the presence of primordial SGWB, which is well motivated from various early universe processes, the above analysis can be interpreted as a measurement of a combined signal of the extragalactic BWD foreground and the primordial SGWB.

Estimating the Primordial SGWB.—The discussion in the previous section provides a way to constrain

$H_P(f) + H_{\text{BWD}}^{\text{ext}}(f)$. In order to measure the primordial component $H_P(f)$ to probe the early universe, the shape of $H_{\text{BWD}}^{\text{ext}}(f)$ must be known with certain precision. Unlike BBHs, BWDs of various masses and types may merge in the LISA band so that the mass distribution may have explicit frequency dependence. The resulting stochastic background deviates from simple power laws at high frequencies (see Fig. 2). A detailed theoretical study can be found in [38]. In this work, instead of using the prediction of [38], we propose to reconstruct the shape of $H_{\text{BWD}}^{\text{ext}}(f)|_{f>5 \text{ mHz}}$ from the individually resolved galactic BWDs. According to Ref. [58], $\sim 10^4$ galactic BWDs in the frequency range (5, 120) mHz are expected to be resolved in the LISA mission time, from which we can reconstruct the spectral density $H_{\text{BWD}}^{\text{ext}}(f)$ (orange dashed line in the upper panel of Fig. 2) with some uncertainty (green shadow) (see Appendix). The reconstruction uncertainty is small at low frequencies where a large number of BWDs reside. However, this method relies on the assumption that the population of galactic BWDs does not deviate significantly from average extragalactic BWDs. This assumption may be tested with population synthesis studies and further examined by comparing the observationally reconstructed background with the prediction in [38].

For illustration purpose, we consider an example with SGWB generated by bubble collisions during a first order phase transition [65]:

$$H_P(f) \sim \frac{10^{-42}}{1 + (f/0.01\text{Hz})^4} \text{ Hz}^{-1}. \quad (6)$$

Without the foreground cleaning, even if we roughly know the spectral shape of $H_{\text{BBH}}(f)$, $H_{\text{BWD}}^{\text{ext}}(f)$, the sensitivity on primordial waves is negligible because of their amplitude ambiguities (see dashed lines in Fig. 3). However, after removing the compact binary foreground, we find that the sensitivity to the primordial waves is greatly enhanced beyond one order of magnitude. The measurement of compact binary foreground and associated multi-band cleaning becomes the critical factor that enables the detection of primordial waves. The reconstruction uncertainty of the extragalactic BWD foreground $H_{\text{BWD}}^{\text{ext}}(f)$ degrades the LISA sensitivity by 5% \sim 50% depending on the LISA running time,

Discussion.— For all the estimators, we have assumed an BBH foreground with a simple power-law spectral density $H_A(f) \propto f^{-7/3}$, which is true only if binaries have zero eccentricity. In the case of mildly eccentric binaries, the spectral density has a more complicated frequency dependence, which deviates from the simple power-law by $\lesssim 50\%$ for BBHs with eccentricity $e \lesssim 0.2$ [66, 67]. In addition, highly eccentric binaries formed through direct captures [68], as sources for ground-based detectors, are born above the LISA band. Therefore it is important to understand the eccentricity distribution of

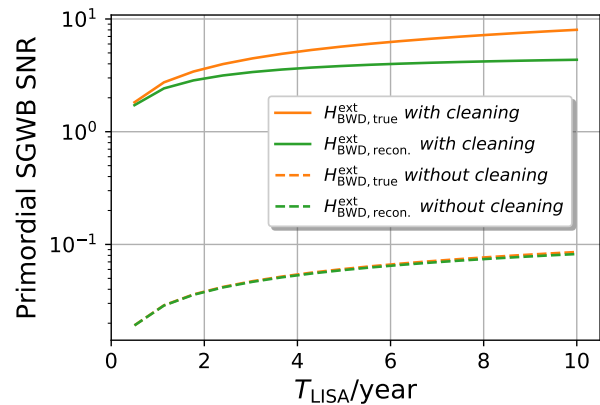


FIG. 3. Measuring the SGWB $H_P(f)$. SNRs of different estimators for the fiducial primordial SGWB, assuming $H_{\text{BWD}}^{\text{ext}}(f)$ is either known (orange) or to be reconstructed (green).

the BBHs for correctly determining the foreground spectral density in the LISA band.

Currently it is believed that there are two main formation channels: field binary evolution and dynamical formation in a dense stellar environment. While BBHs from the former channel are expected to have negligible eccentricities, dynamical formation has the potential to produce BBHs with high eccentricities. As implied by simulations done in Refs. [68, 69], a non-negligible fraction ($\sim 28\% \times 20\% = 5.6\%$) of dynamically formed BBHs in dense globular clusters have large eccentricities ($e_{0.01 \text{ Hz}} \gtrsim 0.1$ or $e_{10 \text{ Hz}} \gtrsim 10^{-4}$) in the LISA band, and a even larger fraction ($\sim 12\%$) of BBHs are born with larger eccentricities ($e_{10 \text{ Hz}} \gtrsim 10^{-3}$) and never enter the LISA band. The latter ones can be readily measured by CE/ET which can distinguish mergers with eccentricities $e_{10 \text{ Hz}} \geq 1.7 \times 10^{-4}$ [70], so that they will not affect the foreground estimation. As a result, we expect $H_A(f)$ to have $\sim 0.5 \times 5.6\% \times F_{\text{dy}}$ deviation from the circular approximation, where F_{dy} is the fraction of BBHs born in the dynamical channel. If dynamical formation is a sub-dominant channel (say, $F_{\text{dy}} < 0.4$), the deviation is likely at sub-percent level and can be safely ignored for our purpose. On the other hand, the loud BBH events detected by LISA may also provide us information about eccentricity distribution in the LISA band [67, 71–73]. Last but not least, another space-borne detector Tianqin is designed to be more sensitive to GWs at higher frequencies (than that of LISA)[74] where the astrophysical foreground is weaker, therefore we expect Tianqin to open another window to probing the primordial SGWB.

Acknowledgements. This research was supported by the Natural Sciences and Engineering Research Council of Canada and in part by Perimeter Institute for Theo-

retical Physics. Research at Perimeter Institute is supported in part by the Government of Canada through the Department of Innovation, Science and Economic Development Canada and by the Province of Ontario through the Ministry of Economic Development, Job Creation and Trade.

* zpan@perimeterinstitute.ca

† hyang@perimeterinstitute.ca

- [1] C. Caprini and D. G. Figueroa, *Classical and Quantum Gravity* **35**, 163001 (2018), [arXiv:1801.04268](https://arxiv.org/abs/1801.04268).
- [2] N. Christensen, *Reports on Progress in Physics* **82**, 016903 (2019), [arXiv:1811.08797](https://arxiv.org/abs/1811.08797) [gr-qc].
- [3] A. H. Guth, *Phys. Rev. D* **23**, 347 (1981).
- [4] A. D. Linde, *Physics Letters B* **108**, 389 (1982).
- [5] A. A. Starobinskiĭ, *Soviet Journal of Experimental and Theoretical Physics Letters* **30**, 682 (1979).
- [6] M. S. Turner, *Phys. Rev. D* **55**, R435 (1997).
- [7] R. Easther and E. A. Lim, *JCAP* **4**, 010 (2006), [astro-ph/0601617](https://arxiv.org/abs/hep-ph/0601617).
- [8] R. Easther, J. T. Giblin, and E. A. Lim, *Phys. Rev. Lett.* **99**, 221301 (2007).
- [9] N. Barnaby, E. Pajer, and M. Peloso, *Phys. Rev. D* **85**, 023525 (2012).
- [10] J. L. Cook and L. Sorbo, *Phys. Rev. D* **85**, 023534 (2012).
- [11] T. W. B. Kibble, *Journal of Physics A Mathematical General* **9**, 1387 (1976).
- [12] A. Vilenkin, *Physics Letters B* **107**, 47 (1981).
- [13] C. J. Hogan and M. J. Rees, *Nature (London)* **311**, 109 (1984).
- [14] R. R. Caldwell and B. Allen, *Phys. Rev. D* **45**, 3447 (1992).
- [15] A. Vilenkin and E. P. S. Shellard, *Cosmic strings and other topological defects*, Cambridge: Cambridge University Press (1994).
- [16] T. Damour and A. Vilenkin, *Phys. Rev. Lett.* **85**, 3761 (2000), [arXiv:gr-qc/0004075](https://arxiv.org/abs/gr-qc/0004075) [gr-qc].
- [17] T. Damour and A. Vilenkin, *Phys. Rev. D* **64**, 064008 (2001), [arXiv:gr-qc/0104026](https://arxiv.org/abs/gr-qc/0104026) [astro-ph].
- [18] R. Jeannerot, J. Rocher, and M. Sakellariadou, *Phys. Rev. D* **68**, 103514 (2003).
- [19] T. Damour and A. Vilenkin, *Phys. Rev. D* **71**, 063510 (2005).
- [20] M. Sakellariadou, *Annalen der Physik* **15**, 264 (2006).
- [21] M. Sakellariadou, in *Lecture Notes in Physics*, Berlin Springer Verlag, Vol. 718, edited by W. G. Unruh and R. Schützhold (2007) p. 247, [hep-th/0602276](https://arxiv.org/abs/hep-th/0602276).
- [22] X. Siemens, V. Mandic, and J. Creighton, *Phys. Rev. Lett.* **98**, 111101 (2007).
- [23] M. S. Turner and F. Wilczek, *Phys. Rev. Lett.* **65**, 3080 (1990).
- [24] M. S. Turner, E. J. Weinberg, and L. M. Widrow, *Phys. Rev. D* **46**, 2384 (1992).
- [25] A. Kosowsky, M. S. Turner, and R. Watkins, *Phys. Rev. D* **45**, 4514 (1992).
- [26] A. Kosowsky, M. S. Turner, and R. Watkins, *Phys. Rev. Lett.* **69**, 2026 (1992).
- [27] M. Kamionkowski, A. Kosowsky, and M. S. Turner, *Phys. Rev. D* **49**, 2837 (1994).
- [28] C. Caprini, R. Durrer, and G. Servant, *Phys. Rev. D* **77**, 124015 (2008).
- [29] S. Iso, P. D. Serpico, and K. Shimada, *Phys. Rev. Lett.* **119**, 141301 (2017).
- [30] D. Cutting, M. Hindmarsh, and D. J. Weir, *Phys. Rev. D* **97**, 123513 (2018), [arXiv:1802.05712](https://arxiv.org/abs/1802.05712) [astro-ph.CO].
- [31] M. Kamionkowski, A. Kosowsky, and A. Stebbins, *Phys. Rev. Lett.* **78**, 2058 (1997).
- [32] U. Seljak and M. Zaldarriaga, *Phys. Rev. Lett.* **78**, 2054 (1997).
- [33] G. Hobbs, A. Archibald, Z. Arzoumanian, D. Backer, M. Bailes, N. D. R. Bhat, M. Burgay, S. Burke-Spolaor, D. Champion, I. Cognard, W. Coles, J. Cordes, P. Demorest, G. Desvignes, R. D. Ferdman, L. Finn, P. Freire, M. Gonzalez, J. Hessels, A. Hotan, G. Janssen, F. Jenet, A. Jessner, C. Jordan, V. Kaspi, M. Kramer, V. Kondratiev, J. Lazio, K. Lazaridis, K. J. Lee, Y. Levin, A. Lommen, D. Lorimer, R. Lynch, A. Lyne, R. Manchester, M. McLaughlin, D. Nice, S. Osłowski, M. Pilia, A. Possenti, M. Purver, S. Ransom, J. Reynolds, S. Sanidas, J. Sarkissian, A. Sesana, R. Shannon, X. Siemens, I. Stairs, B. Stappers, D. Stinebring, G. Theureau, R. van Haasteren, W. van Straten, J. P. W. Verbiest, D. R. B. Yardley, and X. P. You, *Classical and Quantum Gravity* **27**, 084013 (2010), [arXiv:0911.5206](https://arxiv.org/abs/0911.5206) [astro-ph.SR].
- [34] P. L. Bender, A. Brillet, I. Ciufolini, A. M. Cruise, C. J. Cutler, K. Danzmann, F. Fidecaro, W. M. Folkner, J. H. Hough, P. A. Mcnamara, M. Peterseim, D. I. Robertson, M. R. e Rodrigues, A. Ruediger, M. Sandford, R. Schilling, B. Schutz, C. C. Speake, R. T. Stebbins, T. J. Sumner, P. Touboul, J.-Y. Vinet, S. Vitale, H. Ward, and W. Winkler, “LISA Pre-Phase A Report,” (1998).
- [35] S. Sato, S. Kawamura, M. Ando, T. Nakamura, K. Tsubono, A. Araya, I. Funaki, K. Ioka, N. Kanda, S. Moriwaki, M. Musha, K. Nakazawa, K. Numata, S.-i. Sakai, N. Seto, T. Takashima, T. Tanaka, K. Agatsuma, K.-s. Aoyanagi, K. Arai, H. Asada, Y. Aso, T. Chiba, T. Ebisuzaki, Y. Ejiri, M. Enoki, Y. Eriguchi, M.-K. Fujimoto, R. Fujita, M. Fukushima, T. Futamase, K. Gzanu, T. Harada, T. Hashimoto, K. Hayama, W. Hikida, Y. Himemoto, H. Hirabayashi, T. Hiramatsu, F.-L. Hong, H. Horisawa, M. Hosokawa, K. Ichiki, T. Ikegami, K. T. Inoue, K. Ishidoshiro, H. Ishihara, T. Ishikawa, H. Ishizaki, H. Ito, Y. Itoh, N. Kawashima, F. Kawazoe, N. Kishimoto, K. Kiuchi, S. Kobayashi, K. Kohri, H. Koizumi, Y. Kojima, K. Kokeyama, W. Kokuyama, K. Kotake, Y. Kozai, H. Kudoh, H. Kunimori, H. Kuninaka, K. Kuroda, K.-i. Maeda, H. Matsuhara, Y. Mino, O. Miyakawa, S. Miyoki, M. Y. Morimoto, T. Morioka, T. Morisawa, S. Mukohyama, S. Nagano, I. Naito, K. Nakamura, H. Nakano, K. Nakao, S. Nakasuka, Y. Nakayama, E. Nishida, K. Nishiyama, A. Nishizawa, Y. Niwa, T. Noumi, Y. Obuchi, M. Ohashi, N. Ohishi, M. Ohkawa, N. Okada, K. Onozato, K. Oohara, N. Sago, M. Saijo, M. Sakagami, S. Sakata, M. Sasaki, T. Sato, M. Shibata, H. Shinkai, K. Somiya, H. Sotani, N. Sugiyama, Y. Suwa, R. Suzuki, H. Tagoshi, F. Takahashi, K. Takahashi, K. Takahashi, R. Takahashi, T. Takahashi, H. Takahashi, T. Akiteru, T. Takano, K. Taniguchi, A. Taruya, H. Tashiro, Y. Torii, M. Toyoshima, S. Tsujikawa, Y. Tsunesada, A. Ueda, K.-i. Ueda, M. Utashima, Y. Wakabayashi, H. Yamakawa, K. Yamamoto, T. Yamazaki, J. Yokoyama, C.-M. Yoo, S. Yoshida, and

- T. Yoshino, in *Journal of Physics Conference Series*, Journal of Physics Conference Series, Vol. 840 (2017) p. 012010.
- [36] The LIGO/Virgo Scientific Collaboration, *Phys. Rev. Lett.* **118**, 121101 (2017).
- [37] P. D. Lasky, C. M. F. Mingarelli, T. L. Smith, J. T. Giblin, E. Thrane, D. J. Reardon, R. Caldwell, M. Bailes, N. D. R. Bhat, S. Burke-Spolaor, S. Dai, J. Dempsey, G. Hobbs, M. Kerr, Y. Levin, R. N. Manchester, S. Osłowski, V. Ravi, P. A. Rosado, R. M. Shannon, R. Spiewak, W. van Straten, L. Toomey, J. Wang, L. Wen, X. You, and X. Zhu, *Phys. Rev. X* **6**, 011035 (2016).
- [38] A. J. Farmer and E. S. Phinney, *MNRAS* **346**, 1197 (2003), [arXiv:astro-ph/0304393](https://arxiv.org/abs/astro-ph/0304393) [astro-ph].
- [39] S. Marassi, R. Schneider, G. Corvino, V. Ferrari, and S. P. Zwart, *Phys. Rev. D* **84**, 124037 (2011).
- [40] P. A. Rosado, *Phys. Rev. D* **84**, 084004 (2011).
- [41] X.-J. Zhu, E. Howell, T. Regimbau, D. Blair, and Z.-H. Zhu, *Astrophys. J.* **739**, 86 (2011), [arXiv:1104.3565](https://arxiv.org/abs/1104.3565) [gr-qc].
- [42] C. Wu, V. Mandic, and T. Regimbau, *Phys. Rev. D* **85**, 104024 (2012).
- [43] X.-J. Zhu, E. J. Howell, D. G. Blair, and Z.-H. Zhu, *MNRAS* **431**, 882 (2013), [arXiv:1209.0595](https://arxiv.org/abs/1209.0595) [gr-qc].
- [44] The LIGO/Virgo Scientific Collaboration (LIGO Scientific Collaboration and Virgo Collaboration), *Phys. Rev. Lett.* **120**, 091101 (2018).
- [45] A. Sesana, *Phys. Rev. Lett.* **116**, 231102 (2016).
- [46] E. Barausse, N. Yunes, and K. Chamberlain, *Physical Review Letters* **116**, 241104 (2016), [arXiv:1603.04075](https://arxiv.org/abs/1603.04075) [gr-qc].
- [47] S. Vitale, *Physical Review Letters* **117**, 051102 (2016), [arXiv:1605.01037](https://arxiv.org/abs/1605.01037) [gr-qc].
- [48] M. Tinto and J. C. N. de Araujo, *Phys. Rev. D* **94**, 081101 (2016), [arXiv:1608.04790](https://arxiv.org/abs/1608.04790) [astro-ph.IM].
- [49] A. Sesana, in *Journal of Physics Conference Series*, Journal of Physics Conference Series, Vol. 840 (2017) p. 012018, [arXiv:1702.04356](https://arxiv.org/abs/1702.04356) [astro-ph.HE].
- [50] K. W. Wong, E. D. Kovetz, C. Cutler, and E. Berti, *Phys. Rev. Lett.* **121**, 251102 (2018).
- [51] S. Isoyama, H. Nakano, and T. Nakamura, *Progress of Theoretical and Experimental Physics* **2018**, 073E01 (2018), [arXiv:1802.06977](https://arxiv.org/abs/1802.06977) [gr-qc].
- [52] Z. Carson and K. Yagi, *arXiv e-prints* (2019), [arXiv:1905.13155](https://arxiv.org/abs/1905.13155) [gr-qc].
- [53] N. Bartolo, C. Caprini, V. Domcke, D. G. Figueroa, J. Garcia-Bellido, M. Chiara Guzzetti, M. Liguori, S. Matarrese, M. Peloso, A. Petiteau, A. Ricciardone, M. Sakellariadou, L. Sorbo, and G. Tasinato, *JCAP* **2016**, 026 (2016), [arXiv:1610.06481](https://arxiv.org/abs/1610.06481) [astro-ph.CO].
- [54] B. P. Abbott, R. Abbott, T. D. Abbott, M. R. Abernathy, K. Ackley, C. Adams, P. Addesso, R. X. Adhikari, V. B. Adya, C. Affeldt, and et al., *Classical and Quantum Gravity* **34**, 044001 (2017), [arXiv:1607.08697](https://arxiv.org/abs/1607.08697) [astro-ph.IM].
- [55] M. Punturo et al., *Proceedings, 14th Workshop on Gravitational wave data analysis (GWDAAW-14): Rome, Italy, January 26-29, 2010*, *Class. Quant. Grav.* **27**, 194002 (2010).
- [56] T. Regimbau, M. Evans, N. Christensen, E. Katsavounidis, B. Sathyaprakash, and S. Vitale, *Phys. Rev. Lett.* **118**, 151105 (2017).
- [57] D. Reitze, LIGO Laboratory: California Institute of Technology, LIGO Laboratory: Massachusetts Institute of Technology, LIGO Hanford Observatory, and LIGO Livingston Observatory, *BAAS* **51**, 141 (2019), [arXiv:1903.04615](https://arxiv.org/abs/1903.04615) [astro-ph.IM].
- [58] A. Lamberts, S. Blunt, T. B. Littenberg, S. Garrison-Kimmel, T. Kupfer, and R. E. Sanderson, *MNRAS* **490**, 5888 (2019), [arXiv:1907.00014](https://arxiv.org/abs/1907.00014) [astro-ph.HE].
- [59] The LIGO/Virgo Scientific Collaboration, (2018), [arXiv:1811.12940](https://arxiv.org/abs/1811.12940).
- [60] P. Ajith, M. Hannam, S. Husa, Y. Chen, B. Brügmann, N. Dorband, D. Müller, F. Ohme, D. Pollney, C. Reisswig, L. Santamaría, and J. Seiler, *Phys. Rev. Lett.* **106**, 241101 (2011).
- [61] <https://kdepy.readthedocs.io/en/latest/introduction.html#>.
- [62] The KDE estimator is smoothed over its bandwidth, therefore it does not capture variations with length scale much shorter than the bandwidth.
- [63] The gravitational memory produced in compact binary mergers [75] is much weaker than these sources in the inspiraling stage.
- [64] N. Cornish and T. Robson, in *Journal of Physics Conference Series*, Journal of Physics Conference Series, Vol. 840 (2017) p. 012024, [arXiv:1703.09858](https://arxiv.org/abs/1703.09858) [astro-ph.IM].
- [65] C. Caprini, R. Durrer, T. Konstandin, and G. Servant, *Phys. Rev. D* **79**, 083519 (2009).
- [66] E. A. Huerta, S. T. McWilliams, J. R. Gair, and S. R. Taylor, *Phys. Rev. D* **92**, 063010 (2015), [arXiv:1508.02828](https://arxiv.org/abs/1508.02828) [astro-ph].
- [67] L. Randall and Z.-Z. Xianyu, (2019), [arXiv:1907.02283](https://arxiv.org/abs/1907.02283).
- [68] C. L. Rodriguez, P. Amaro-Seoane, S. Chatterjee, K. Kremer, F. A. Rasio, J. Samsing, C. S. Ye, and M. Zevin, *Phys. Rev. D* **98**, 123005 (2018).
- [69] K. Kremer, C. L. Rodriguez, P. Amaro-Seoane, K. Breivik, S. Chatterjee, M. L. Katz, S. L. Larson, F. A. Rasio, J. Samsing, C. S. Ye, and M. Zevin, *Phys. Rev. D* **99**, 63003 (2019).
- [70] M. E. Lower, E. Thrane, P. D. Lasky, and R. Smith, *Phys. Rev. D* **98**, 083028 (2018).
- [71] K. Breivik, C. L. Rodriguez, S. L. Larson, V. Kalogera, and F. A. Rasio, *Astrophys. J.* **830**, L18 (2016).
- [72] A. Nishizawa, E. Berti, A. Klein, and A. Sesana, *Phys. Rev. D* **94**, 064020 (2016).
- [73] A. Nishizawa, A. Sesana, E. Berti, and A. Klein, *Mon. Not. R. Astron. Soc.* **465**, 4375 (2017), [arXiv:1606.09295](https://arxiv.org/abs/1606.09295).
- [74] X.-Y. Lu, Y.-J. Tan, and C.-G. Shao, *Phys. Rev. D* **100**, 044042 (2019).
- [75] H. Yang and D. Martynov, *Phys. Rev. Lett.* **121**, 071102 (2018), [arXiv:1803.02429](https://arxiv.org/abs/1803.02429) [gr-qc].
- [76] B. Allen and J. D. Romano, *Phys. Rev. D* **59**, 102001 (1999), [arXiv:9710117](https://arxiv.org/abs/9710117) [gr-qc].
- [77] E. S. Phinney, “A practical theorem on gravitational wave backgrounds,” (2001), [arXiv:astro-ph/0108028](https://arxiv.org/abs/astro-ph/0108028) [astro-ph].
- [78] C. Cutler and É. E. Flanagan, *Phys. Rev. D* **49**, 2658 (1994).
- [79] S. Cole, P. Norberg, C. M. Baugh, C. S. Frenk, J. Bland-Hawthorn, T. Bridges, R. Cannon, M. Colless, C. Collins, W. Couch, N. Cross, G. Dalton, R. De Propris, S. P. Driver, G. Efstathiou, R. S. Ellis, K. Glazebrook, C. Jackson, O. Lahav, I. Lewis, S. Lumsden, S. Maddox, D. Madgwick, J. A. Peacock, B. A. Peterson, W. Sutherland, and K. Taylor, *MNRAS* **326**, 255 (2001),

arXiv:astro-ph/0012429 [astro-ph].

- [80] N. J. Cornish and S. L. Larson, *Class. Quantum Gravity* **18**, 3473 (2001).
 [81] N. J. Cornish, *Phys. Rev. D* **65**, 022004 (2001).
 [82] R. W. Hellings and W. A. Hiscock, *Phys. Rev. D - Part. Fields, Gravit. Cosmol.* **62**, 062001 (2000).
 [83] J. D. Romano and N. J. Cornish, *Living Reviews in Relativity* **20** (2017), 10.1007/s41114-017-0004-1.
 [84] J. W. Armstrong, F. B. Estabrook, and M. Tinto, *Astrophys. J.* **527**, 814 (1999).
 [85] M. Tinto, J. W. Armstrong, and F. B. Estabrook, *Phys. Rev. D* **63**, 021101 (2000).
 [86] C. J. Hogan and P. L. Bender, *Phys. Rev. D* **64**, 062002 (2001), astro-ph/0104266.
 [87] T. Robson, N. Cornish, and C. Liug, *Class. Quantum Gravity* **36**, 105011 (2018), arXiv:1803.01944.

Stochastic GWs From Binary Black Holes

Assuming the SGWB is isotropic, unpolarized and stationary, we can define its spectral density $H(f)$ as (our definition is different from that of Ref. [76] by a factor 8π),

$$\langle h_A^*(f, \hat{\Omega}) h_B(f', \hat{\Omega}') \rangle = \frac{1}{2} \frac{\delta_{\hat{\Omega}, \hat{\Omega}'}}{4\pi} \delta_{AB} \delta(f - f') H(f), \quad (7)$$

with $h_A(f, \hat{\Omega})$ being the waveform of gravitational waves coming from direction $\hat{\Omega}$ with polarization state $A \in \{+, \times\}$ written in the Fourier domain. The spectral density $H(f)$ is related to the energy density of the SGWB by

$$\rho_{\text{GW}} = \frac{\pi}{2} \int_0^\infty f^2 H(f) df, \quad (8)$$

which in turn relates to the energy fraction of GWs in a logarithmic frequency bin $\Omega_{\text{GW}}(f)$ by

$$\Omega_{\text{GW}}(f) := \frac{1}{\rho_{\text{crit}}} \frac{d\rho_{\text{GW}}}{d \ln f} = \frac{4\pi^2}{3H_0^2} |f|^3 H(|f|), \quad (9)$$

where $\rho_{\text{crit}} := 3H_0^2/8\pi$ is critical energy density to close the universe.

The energy density of GWs averaged over all inspiral binaries in different directions $\hat{\Omega}$ and a period of time $[-T/2, T/2]$ is [77]

$$\begin{aligned} \hat{\rho}_{\text{GW}} &= \frac{1}{T} \sum_i \int_{-T/2}^{T/2} S_i(t) dt \\ &= \frac{1}{T} \sum_i \int_{-T/2}^{T/2} \frac{1}{16\pi} (\dot{h}_+^2 + \dot{h}_\times^2)_i dt \\ &= \frac{\pi}{2T} \sum_i \int_{f_-^i}^{f_+^i} f^2 (|h_+(f)|^2 + |h_\times(f)|^2)_i df, \end{aligned} \quad (10)$$

with index i running over all BBHs in the universe, $S_i(t)$ being the energy flux of GWs emitted by the i -th BBH,

dots denoting time derivative and $f_\pm^i = f^i|_{t=\pm T/2}$ being the GW frequency of i -th BBH at $t = \pm T/2$. According to Eqs.(8) and (10), we find the spectral density of the BBH foreground averaged over time period $[-T/2, T/2]$ is

$$\hat{H}_A(f) = \frac{1}{T} \sum_i (|h_+(f)|^2 + |h_\times(f)|^2)_i \Theta_T^i(f), \quad (11)$$

where $\Theta_T^i(f) = 1$ if $f \in [f_-^i, f_+^i]$ and $\Theta_T^i(f) = 0$ otherwise.

To obtain the mean value of $\hat{H}_A(f)$, we first consider a sample of BBHs with same redshift z_s , same chirp mass M_s and merger rate \dot{N}_s . For this sample, all BBHs evolve along the same frequency-time curve $f(t - t_{\text{merger}}^i)$, i.e., $\frac{1}{T} \langle \sum_s \Theta_T^s(f) \rangle$ is independent of frequency f (as long as f is lower than the merger frequency) and is equal to \dot{N}_s . Therefore, we have

$$\langle \hat{H}_A(f) \rangle_s = \langle (|h_+(f)|^2 + |h_\times(f)|^2)_s \rangle \times \dot{N}_s. \quad (12)$$

Now consider BBHs in the real universe, with a merger rate density $R(z)$ (number of mergers per comoving volume per unit of cosmic time local to the event) and the chirp mass distribution $p(M_c)$, we have the merger rate $\dot{N}_s(z, M_c) dz dM_c = \frac{R(z)}{1+z} dV_c(z) p(M_c) dM_c$ and the mean value of $\hat{H}_A(f)$ [77]

$$\langle \hat{H}_A(f) \rangle = \int_0^\infty \int_{M_{c,\min}}^{M_{c,\max}} \langle \sum_A |h_A(f)|_s^2 \rangle \dot{N}_s dz dM_c, \quad (13)$$

where $dV_c(z) = 4\pi r^2(z)/H(z) dz$ is the comoving volume element, with $r(z) = \int_0^z dz/H(z)$ being the comoving radial distance and $H(z)$ being the Hubble expansion rate at redshift z . In the quasi-circular approximation, the waveform in the LISA band is [e.g., 78]

$$\begin{aligned} h_+(f) &= \frac{1 + \cos^2 \iota}{2} \sqrt{\frac{5}{24}} \frac{(GM_z)^{5/6} f^{-7/6}}{\pi^{2/3} D_L} e^{-i\Psi(f)}, \\ h_\times(f) &= i \cos \iota \sqrt{\frac{5}{24}} \frac{(GM_z)^{5/6} f^{-7/6}}{\pi^{2/3} D_L} e^{-i\Psi(f)}, \end{aligned} \quad (14)$$

where ι is the inclination angle of the binary with respect to observers on the earth, $\mathcal{M}_z = (1+z)M_c$ is the redshifted chirp mass, D_L is the luminosity distance and $\Psi(f)$ is the wave phase. Plugging Eq. (14) into Eq. (13), we find

$$\langle \hat{H}_A(f) \rangle = \dot{N}_O \frac{f^{-7/3}}{6\pi^{4/3}} \int_0^\infty P(\zeta) \zeta^2 d\zeta, \quad (15)$$

where

$$\dot{N}_O = \int_0^\infty \int_{M_{c,\min}}^{M_{c,\max}} \dot{N}_s(z, M_c) dz dM_c,$$

is the merger rate seen in the observer's frame, $\zeta = (GM_z)^{5/6}/D_L$ and $P(\zeta)$ is the corresponding probability distribution.

BBH Foreground cleaning by event-based subtraction

In the main text, we reconstructed the underlying distribution of BBH mergers from all the mergers recorded by the CE following the statistical approach. Now we explore the foreground measurement of event-to-event approach. Assume the LISA runs from $-T/2$ to $T/2$, and the CE runs from $-T/2$ to $-T/2 + T_{\text{CE}}$. For each BBH in the LISA band, we expect to detect its merger after some time t in the CE band, where t is determined by the GW frequency evolution equation [see e.g., Ref. 78]

$$\frac{dt}{df} = \frac{5}{96\pi^{8/3}} \frac{f^{-11/3}}{[GM_c(1+z)]^{5/3}}, \quad (16)$$

and we can add up the contribution to the LISA band foreground from BBHs which merger during the CE running phase,

$$\hat{H}_A(f)|_{\text{CE}} = \frac{1}{T} \sum_j (|h_+(f)|^2 + |h_\times(f)|^2)_j \Theta_T^j(f) df,$$

where j runs over all mergers detected by the CE. If the CE runs for a infinitely long time $T_{\text{CE}} \rightarrow \infty$, $\hat{H}_A(f)|_{\text{CE}} \rightarrow \hat{H}_A(f)$. For a finite CE running time, only a fraction of BBHs in the LISA band will evolve into merger phase and the expectation value turns out to be

$$\begin{aligned} \langle \hat{H}_A(f)|_{\text{CE}} \rangle &= \int_{z=z_{\min}(f, M_c)}^{z=\infty} \int_{M_{c,\min}}^{M_{c,\max}} \sum_A |h_A(f)|^2 \\ &\times \frac{R(z)}{1+z} dV_c(z) p(M_c) dM_c, \end{aligned} \quad (17)$$

where $z_{\min}(f, M_c)$ is determined by Eq. (16)

$$T_{\text{CE}} = \frac{15}{768\pi^{8/3}} \frac{f^{-8/3}}{[GM_c(1+z_{\min})]^{5/3}}, \quad (18)$$

where we have used the fact that the BBH merger frequency is well above the LISA band frequency f .

In Fig. 4, we show the residue fraction after the event-to-event cleaning $1 - \langle \hat{H}_A(f)|_{\text{CE}} \rangle / \langle \hat{H}_A(f) \rangle$ given a finite running CE time ($T_{\text{CE}} = 10, 20, 30$ years). It takes longer time for binaries of lower frequency to merge, therefore lower-frequency foreground cleaning is slower. With the CE running for 10 years, the astrophysical foreground can be cleaned to percent level for $f \gtrsim 0.03$ Hz. Therefore the foreground cleaning of distribution-based approach is more efficient than that of event-based approach.

Stochastic GWs from Binary White Dwarfs

Similar to BBHs, the spectral density of the Binary White Dwarf (BWD) foreground averaged over time period $[-T/2, T/2]$ is also

$$\hat{H}_{\text{BWD}}(f) = \frac{1}{T} \sum_i (|h_+(f)|^2 + |h_\times(f)|^2)_i \Theta_T^i(f), \quad (19)$$

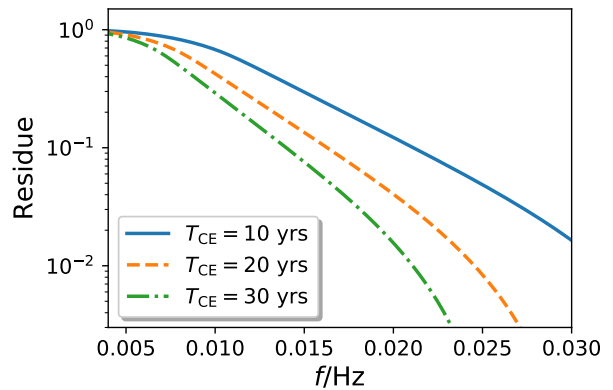


FIG. 4. Performance of foreground cleaning with event-based subtraction.

where f is a frequency in the LISA band. Unlike BBHs, BWDs merge in the LISA band, and this results in some frequency dependence of the expectation value $\langle \frac{1}{T} \sum_i \Theta_T^i(f) \rangle$. This extra frequency dependence drives $H_{\text{BWD}}(f)$ off the power law $f^{-7/3}$ and it is hard to calculate from first principle.

According to simulations performed in Ref. [58], all the high-frequency (say $f > 5$ mHz) galactic BWDs are expected to be resolved in the LISA mission time. From these BWDs, we can construct a normalized spectral density,

$$H_D(f) \propto \frac{1}{T} \sum_i \left(\sum_A |h_A(f)|^2 D_{\text{L,eff}}^2 \right)_i \Theta_T^i(f), \quad (20)$$

where all the effective distance information has been removed, $D_{\text{L,eff}} = D_L / \sqrt{\cos^2 \iota + (\frac{1+\cos^2 \iota}{2})^2}$. The normalized spectral density $H_D(f)$ is actually a statistical property of the galactic BWDs and can be used to reconstruct the extragalactic BWD foreground if the population of galactic BWDs does not deviate significantly from average extragalactic BWDs. The spectral density of extragalactic BWD foreground is then calculated as

$$H_{\text{BWD}}^{\text{ext}}(f) \propto \int_0^{V_c(z_*)} \frac{H_D(f(1+z))}{D_L^2(z)} \frac{\mathcal{F}(z)}{1+z} dV_c(z), \quad (21)$$

where $\mathcal{F}(z)$ is the formation rate of high-frequency BWDs. Though the accurate form of $\mathcal{F}(z)$ is unknown, as we will show later, it has little influence on the shape of $H_{\text{BWD}}^{\text{ext}}(f)$.

There are two major sources of the uncertainty of $H_{\text{BWD}}^{\text{ext}}(f)$ reconstruction from resolvable galactic BWDs, one is statistic uncertainty due to limited number of galactic BWDs and the other is the uncertainty in the formation rate $\mathcal{F}(z)$. Following [58], we assume the total number of resolvable high-frequency galactic BWDs is 10^4 , and these BWDs roughly satisfy a power-law distribution $dN/df \propto f^{-4.8}$ in the frequency range [5, 120]

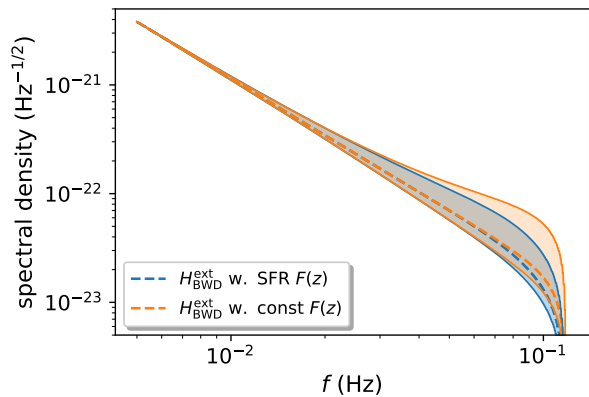


FIG. 5. The shape of spectral density $H_{\text{BWD}}^{\text{ext}}(f)$ is insensitive to the formation rate $\mathcal{F}(z)$ of high-frequency BWDs. The solid line is the result of setting $F(z)$ equal to the star formation rate derived in [79], and the dashed line is the result of constant $F(z)$ (we have normalized the amplitude of $H_{\text{BWD}}^{\text{ext}}(f)$ at low frequency). The blue and orange shadows are the corresponding statistic uncertainties of reconstruction from limited number of resolvable galactic BWDs.

mHz. For the chirp mass, we assume a Gaussian distribution with mean value $0.4M_{\odot}$ and standard deviation $0.1M_{\odot}$. To examine how much uncertainty in $H_{\text{BWD}}^{\text{ext}}(f)$ is introduced by the uncertainty of $\mathcal{F}(z)$, we consider two $\mathcal{F}(z)$ functions: one is the star formation rate derived in Ref. [79], and the other is a constant. For each $F(z)$, we simulate 100 realizations of resolved galactic BWDs, for each of which we fit $\log H_D - \log f$ with a 2nd-degree polynomial and calculate $H_{\text{BWD}}^{\text{ext}}(f)$ from Eq. (21). The true spectral density $H_{\text{BWD}}^{\text{ext}}(f)$ along with the reconstruction uncertainties are shown in Fig. 5, which clearly shows the shape of $H_{\text{BWD}}^{\text{ext}}(f)$ is insensitive to $\mathcal{F}(z)$ and the reconstruction uncertainty is dominated by the statistic uncertainty.

Estimator of extragalactic Binary White Dwarf Background

For simplicity, let us consider two LISA detectors with output $s_d(t) = h_d(t) + n_d(t)$ ($d = 1, 2$), with h_d and n_d denoting the gravitational strain and the intrinsic noise in detector d , respectively. The SGWs signal can be measured by cross-correlating outputs from two detector because the detector noises n_1 and n_2 are not correlated, while the GW signals h_1 and h_2 are correlated. In the Fourier domain, the cross-correlation estimator is written as [76]

$$\hat{X} = \int_{-\infty}^{\infty} df \int_{-\infty}^{\infty} df' \delta_T(f - f') s_1^*(f) s_2(f') Q(f), \quad (22)$$

where $\delta_T(f) := \sin(\pi f T) / (\pi f)$ is a finite-time approximation to the δ -function, T is the running time of the

two detectors and $Q(f)$ is a filter function. For later convenience, we define

$$\begin{aligned} \langle H_x(f) \rangle_a^b &:= \int_a^b H_x(f) \mathcal{R}_{12}(f) Q(f) df, \\ \langle H_x(f) \rangle_{[a,b]}^{[b,c]} &:= \langle H_x(f) \rangle_a^b - \langle H_x(f) \rangle_b^c, \end{aligned} \quad (23)$$

where

$$\mathcal{R}_{12}(f) = \int \frac{d\hat{\Omega}}{4\pi} e^{i2\pi f(\hat{x}_1 - \hat{x}_2) \cdot \hat{\Omega}} \sum_A F_1^{A*}(\hat{\Omega}, f) F_2^A(\hat{\Omega}, f),$$

is the overlap reduction function of the two detectors which we assume form a hexagonal pattern. The mean value and variance of estimator \hat{X} turn out to be [76]

$$\begin{aligned} \langle \hat{X} \rangle &= T \langle H(f) \rangle_0^\infty, \\ \sigma_{\hat{X}}^2 &\approx \frac{T}{2} \int_0^\infty P_n^2(f) |Q(f)|^2 df, \end{aligned} \quad (24)$$

where $P_n(f)$ is the detector noise spectral density [34, 80–82]. In the ideal case of zero foreground, we can extract the primordial signal directly using the estimator (24). With the optimal filter $Q(f) = H(f) \mathcal{R}_{12}^*(f) / P_n^2(f)$, we obtain the maximized signal-to-noise ratio (SNR)

$$\text{SNR}_{\text{ideal}} = \sqrt{2T \int_0^\infty \frac{H^2(f)}{P_n^2(f)} |\mathcal{R}_{12}(f)|^2 df}. \quad (25)$$

The presence of astrophysical foreground of BBHs and galactic BWDs makes the problem more complicated. In the LISA band, the foreground is dominated by the GW emission from galactic BWDs, of which high-frequency binaries can be completely resolved and subtracted in the LISA mission time [58]. And we need to design an estimator with the BBHs foreground subtracted using the KDE reconstruction. The spectral density $H_A(f)$ of the BBH foreground is known as a power law, while the spectral density of galactic BWD foreground depends on their orbital distributions. In the following discussion, we will confine our analysis to the frequency range $f \geq f_{\text{min}} = 5$ mHz, where galactic BWD foreground can be cleaned up and $H(f) \simeq H_{\text{BWD}}^{\text{ext}}(f) + H_A(f)$ to a good approximation.

The spectral density of the astrophysical foreground $H_A(f)$ can be estimated with $H_{\text{kde}}(f)$ elaborated in the main text. From Eq. (24), we define an estimator of the extragalactic BWD foreground as

$$\hat{Y} = \hat{X} - T \langle H_{\text{kde}}(f) \rangle_{f_{\text{min}}}^{f_{\text{max}}}, \quad (26)$$

with expectation value and variance

$$\begin{aligned} \langle \hat{Y} \rangle &= Y_{\text{BWD}}^{\text{ext}} + T \langle H_A(f) - H_{\text{kde}}(f) \rangle_{f_{\text{min}}}^{f_{\text{max}}}, \\ \sigma_{\hat{Y}}^2 &= \frac{T}{2} \int_0^\infty P_n^2(f) |Q(f)|^2 df, \end{aligned} \quad (27)$$

where $Y_{\text{BWD}}^{\text{ext}} = T \langle H_{\text{BWD}}^{\text{ext}}(f) \rangle_0^\infty$ and $f_{\text{max}} = 1$ Hz. Therefore we have $Y_{\text{BWD}}^{\text{ext}} = \hat{Y} + \mathcal{N}(0, \sigma_Y) + \mathcal{N}(0, \sigma_A)$, where $\sigma_Y \propto \sqrt{T}$ is the statistical uncertainty due to detector noise and $\sigma_A = T \langle \sigma_{\text{kde}} H_A(f) \rangle_0^\infty$ is the systematic bias due to the limited accuracy of the foreground measurement. Consequently, the SNR of estimator \hat{Y} , $\text{SNR}_{\hat{Y}} = Y_{\text{BWD}}^{\text{ext}} / \sqrt{\sigma_Y^2 + \sigma_A^2}$, scales as \sqrt{T} for small T , and saturates at $Y_{\text{BWD}}^{\text{ext}} / \sigma_A$ in the large T limit.

Without the multi-band measurement, the influence of BBH foreground may be removed by using its frequency dependence. For later convenience, we first define a binned estimator

$$\hat{X}_{\mathcal{C}} := \int_{f \in \mathcal{C}} df \int_{f' \in \mathcal{C}} df' \delta_T(f-f') s_1^*(f) s_2(f') Q(f), \quad (28)$$

and also define an estimator \hat{Z} :

$$\hat{Z} = \hat{X}_{\mathcal{C}_1} - \hat{X}_{\mathcal{C}_2}, \quad (29)$$

where $\mathcal{C}_1 = [f_{\text{min}}, f_*]$, $\mathcal{C}_2 = [f_*, f_{\text{max}}]$, and f_* is determined by the constraint that the influence of astrophysical foreground is removed $\langle H_A(f) \rangle_{\mathcal{C}_1}^{\mathcal{C}_2} = 0$. The mean value and the variance of \hat{Z} are

$$\begin{aligned} \langle \hat{Z} \rangle &= T \langle H_{\text{BWD}}^{\text{ext}}(f) \rangle_{\mathcal{C}_1}^{\mathcal{C}_2}, \\ \sigma_{\hat{Z}}^2 &= \frac{T}{2} \int_{f_{\text{min}}}^{f_{\text{max}}} P_n^2(f) |Q(f)|^2 df. \end{aligned} \quad (30)$$

In the lower panel of Fig. 2 in the main text, we show the SNRs of estimators defined in Eqs. (26, 29) for the extragalactic BWD SGWs with fiducial spectral density $H_{\text{BWD}}^{\text{ext}}(f)$. For comparison, we also show the SNR of the ideal estimator where there was no foreground contamination.

Estimators of Primordial SGWB

In the presence of primordial SGWB, the estimators defined in the previous section provide a way to measure a combined signal of the extragalactic BWD foreground and the primordial SGWB, $H_{\text{P}}(f) + H_{\text{BWD}}^{\text{ext}}(f)$. In order to constrain the primordial component $H_{\text{P}}(f)$, the shape of $H_{\text{BWD}}^{\text{ext}}(f)$ must be known with certain precision, which can be reconstructed from resolvable galactic BWDs (see the 3rd section).

With the shape information of $H_{\text{BWD}}^{\text{ext}}(f)$, we can remove the extragalactic BWD foreground using its frequency dependence. Similar to estimator \hat{Y} , we can define estimator

$$\hat{U} = \hat{X}_{\mathcal{C}_1} - \hat{X}_{\mathcal{C}_2} - T \langle H_{\text{kde}} \rangle_{\mathcal{C}_1}^{\mathcal{C}_2}, \quad (31)$$

where $\mathcal{C}_1 = [f_{\text{min}}, f_*]$, $\mathcal{C}_2 = [f_*, f_{\text{max}}]$, f_* is determined by the constraint that the influence of extragalactic BWD

foreground is removed $\langle H_{\text{BWD, recon}}^{\text{ext}} \rangle_{\mathcal{C}_1}^{\mathcal{C}_2} = 0$. The mean value and the variance of \hat{U} are

$$\begin{aligned} \langle \hat{U} \rangle &= T \langle H_{\text{P}} + H_{\text{BWD}}^{\text{ext}} + H_A - H_{\text{kde}} \rangle_{\mathcal{C}_1}^{\mathcal{C}_2}, \\ \sigma_{\hat{U}}^2 &= \frac{T}{2} \int_{f_{\text{min}}}^{f_{\text{max}}} P_n^2(f) |Q(f)|^2 df, \end{aligned} \quad (32)$$

Similar to estimator \hat{Y} , we have $U_{\text{P}} := T \langle H_{\text{P}} \rangle_{\mathcal{C}_1}^{\mathcal{C}_2} = \hat{U} + \mathcal{N}(0, \sigma_U) + \mathcal{N}(0, \sigma_{\text{BWD}}) + \mathcal{N}(0, \sigma_A)$, where $\sigma_U \propto \sqrt{T}$ is the statistical uncertainty due to detector noise, σ_{BWD} is the variance of $T \langle H_{\text{BWD, recon}}^{\text{ext}} \rangle_{\mathcal{C}_1}^{\mathcal{C}_2}$ and $\sigma_A = T \langle \sigma_{\text{kde}} H_A \rangle_{\mathcal{C}_1}^{\mathcal{C}_2}$. In Fig. 3 of the main text, we show the SNR of estimator \hat{U} , $\text{SNR}_{\hat{U}} = U_{\text{P}} / \sqrt{\sigma_U^2 + \sigma_{\text{BWD}}^2 + \sigma_A^2}$ as a function of LISA running time.

Similar to estimator \hat{Z} , both the influence of the extragalactic BWD foreground and the BBH foreground can be removed via their frequency dependence without multi-band measurement. We can define estimator

$$\hat{V} = \left(\hat{X}_{\mathcal{C}_1} - \hat{X}_{\mathcal{C}_2} \right) - \left(\hat{X}_{\mathcal{C}_3} - \hat{X}_{\mathcal{C}_4} \right), \quad (33)$$

where $\mathcal{C}_{1, \dots, 4}$ are 4 non-overlapped frequency bins and are determined by the constraint that both the extragalactic BWD foreground and the BBH foreground are removed. The mean value and the variance of \hat{V} are

$$\begin{aligned} \langle \hat{V} \rangle &= T \langle H_{\text{P}} + H_{\text{BWD}}^{\text{ext}} \rangle_{\mathcal{C}_1}^{\mathcal{C}_2} - T \langle H_{\text{P}} + H_{\text{BWD}}^{\text{ext}} \rangle_{\mathcal{C}_3}^{\mathcal{C}_4}, \\ \sigma_{\hat{V}}^2 &= \frac{T}{2} \int_{f_{\text{min}}}^{f_{\text{max}}} P_n^2(f) |Q(f)|^2 df, \end{aligned} \quad (34)$$

We have $V_{\text{P}} := T \langle H_{\text{P}} \rangle_{\mathcal{C}_1}^{\mathcal{C}_2} - T \langle H_{\text{P}} \rangle_{\mathcal{C}_3}^{\mathcal{C}_4} = \hat{V} + \mathcal{N}(0, \sigma_V) + \mathcal{N}(0, \sigma_{\text{BWD}})$, where σ_V is the uncertainty due to detector noise and σ_{BWD} is the variance of $T \langle H_{\text{BWD}}^{\text{ext}} \rangle_{\mathcal{C}_1}^{\mathcal{C}_2} - T \langle H_{\text{BWD}}^{\text{ext}} \rangle_{\mathcal{C}_3}^{\mathcal{C}_4}$. The SNR of estimator \hat{V} , $V_{\text{P}} / \sqrt{\sigma_V^2 + \sigma_{\text{BWD}}^2}$ is also shown in Fig. 3 in the main text.

One detector, two channels

In the main text, we have outlined the foreground cleaning with KDE reconstruction assuming two LISA detectors for convenience, where the stochastic GWs can be separated from detector noise by cross-correlating the two detector outputs. For the proposed LISA mission, there will be a single detector and we may detect the SGWB by utilizing the ‘‘null’’ channel which is blind to GW signals for detector noise calibration, in combination with the normal Michelson (m) channel [83]. In reality, a good approximation to the ideal null channel is the symmetrized Sagnac (ss) channel whose response function $\mathcal{R}_{\text{ss}}(f)$ is much smaller than that of the Michelson channel $\mathcal{R}_{\text{m}}(f)$ especially in the lower frequency range

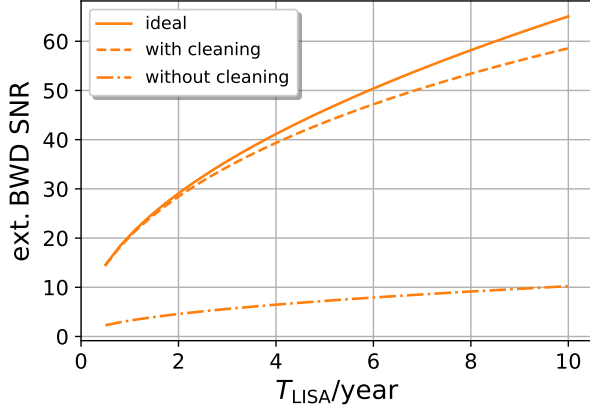


FIG. 6. Measuring the extragalactic BWD foreground using two channels of a single LISA detector.

[81, 84–86]. In combination with the outputs of the two

channels, it is natural to write the SGWB estimator as

$$\hat{X} = \int_{-\infty}^{\infty} df \int_{-\infty}^{\infty} df' \delta_T(f - f') \times [s_m^*(f) s_m(f') - W(f) s_{ss}^*(f) s_{ss}(f')] Q(f), \quad (35)$$

where $W(f) = P_m(f)/P_{ss}(f)$, with $P_{ss}(f)$ and $P_m(f)$ being the detector noise spectral density of two channels [80, 81, 87]. The mean value and variance are

$$\langle \hat{X} \rangle = T \int_0^{\infty} H(f) [\mathcal{R}_m(f) - W(f) \mathcal{R}_{ss}(f)] Q(f) df, \\ \sigma_X^2 \approx 2T \int_0^{\infty} [P_m^2(f) - W(f) |P_{m,ss}(f)|^2] |Q(f)|^2 df.$$

where $P_{m,ss}(f)$ is cross power of noises in the two channels. In the similar way, we can write the estimators \hat{Y} and \hat{Z} as in the case of two LISA detectors. We show the SNRs of different estimators for the extragalactic BWD foreground in Fig. 6. As in the two-detectors case, the BBH foreground cleaning increases the LISA sensitivity by a factor 4 ~ 7. Compared with the case of two detectors, the SNRs of different estimators here turn out to be smaller by a factor ~ 2.